ChemComm

Cite this: *Chem. Commun.*, 2021, **57**, 8624

Received 19th June 2021,
Accepted 2nd August 2021

DOI: 10.1039/d1cc03262c

rsc.li/chemcomm

3d–4f Heterometallic cluster incorporated polyoxoniobates with magnetic properties†

Yu-Diao Lin,[a] Rui Ge,[a] Chong-Bin Tian,[b] Cai Sun,[a] Yan-Qiong Sun,[a] Qing-Xin Zeng,*[a] Xin-Xiong Li*[ab] and Shou-Tian Zheng[a]

A series of 3d–4f heterometallic cluster incorporated polyoxoniobates (PONbs) with different magnetic properties were first made and characterized. This work not only provides a promising strategy to make new heterometallic cluster incorporated PONbs but also demonstrates an ideal model to probe how transition-metal ions influence the magnetic property of PONbs.

Polyoxometalates (POMs), as early transition metal–oxygen clusters of V, Nb, Ta, Mo, and W, have intriguing structural characteristics, such as high negative charge, oxygen-rich surface, and rich redox properties and nanoscale size. Owing to their promising applications in catalysis, medicine, magnetism, and material sciences, there have been constant endeavors to synthesize novel POMs.[1] Notably, metal-substituted POMs (MSPs) have become one of the most researched subclasses of POMs because of their structural diversity and significant applications in magnetism.[2] MSPs are ideal models for the study of magnetic coupling in metal clusters, as they represent a type of well-insulated cluster of distinct nuclearity and particular magnetic coupling models. So far, substantial efforts have been devoted to transition-metal substituted polyoxometalates (TMSPs) and lanthanide substituted polyoxometalates (LSPs), generating a large number of unique MSPs with beautiful architectures and interesting properties.[3]

Nevertheless, compared with the rapidly evolving TMSPs and LSPs, the development of 3d–4f heterometallic cluster incorporated POMs remains far behind, and the number of such materials is still limited.[4] So far, the reported 3d–4f heterometallic cluster incorporated POMs are mainly polyoxotungstates (POTs).[5] For example, Zheng's group obtained two giant 3d–4f incorporated POTs with super-tetrahedral structures, $[LaNi_{12}W_{35}Sb_3P_3O_{139}(OH)_6]^{23-}$ and $[La_{10}Ni_{48}W_{140}Sb_{16}P_{12}O_{568}(OH)_{24}(H_2O)_{20}]^{86-}$.[6] Powell's group reported a high-nuclear 3d–4f cluster incorporated POT $[Dy_{30}Co_8Ge_{12}W_{108}O_{408}(OH)_{42}(OH_2)_{30}]^{56-}$.[7] Moreover, a series of 3d–3d′–4f heptanuclear cluster incorporated POTs ($^{III}FeM_4Ln_2$,$TBA_nH_m[FeM_4\{Ln(L)_2\}_2O_2(A\text{-}\alpha\text{-}SiW_9O_{34})_2]$, M = Mn^{3+}, Cu^{2+}; Ln = Gd^{3+}, Dy^{3+}, Lu^{3+}; L = acac (acetylacetonate), hfac (hexafluoroacetylacetonate), respectively) have been successfully made by Mizuno's group.[8]

PONbs, as an important branch of POMs, have attracted great interest due to their rich structural configurations and promising applications in photocatalysis, base-catalyzed reaction, and decomposition of nerve agents.[9] However, in contrast to 3d–4f heterometallic cluster incorporated POTs, 3d–4f heterometallic incorporated PONbs are hardly ever found. Currently, some PONbs containing both 3d and 4f ions have been made.[10] But, the different ions in these compounds are magnetically isolated from each other by PONb fragments or organic ligands instead of being gathered together to form heterometallic clusters. Therefore, 3d–4f heterometallic cluster incorporated PONbs remain unexplored, probably because of (1) the lack of soluble precursors; (2) the low reaction activity of niobate species; (3) the higher working pH region (pH ≈ 10–12) of PONbs; (4) the incompatibility between niobate species and 3d/4f metal ions under basic conditions. As is well known, the combination of PONbs with different metal ions may open up an opportunity to explore the effects of different metal ions on the performance (magnetism, luminescence, .) of the final materials. Thus, the synthesis of 3d–4f cluster incorporated PONbs remains an ongoing challenge, which needs to be addressed urgently.

Based on the above considerations, the first series of 3d–4f heterometallic cluster incorporated PONbs with a general formula of $Na_6H_{20}\{TM_2[Dy_3O(\mu_3\text{-}OH)_3(H_2O)_3]_2(Nb_6O_{19})_5\}\cdot H_2O$ (**1-TM-Dy**, TM = Cr, Mn, Fe, Co, for = 62, 63, 63, 56, respectively) have been obtained. The crystals of **1-TM-Dy** are presented in Fig. 1. To the best of our knowledge, **1-TM-Dy** represent the first examples of 3d–4f heterometallic cluster incorporated PONbs. More interestingly, it is found that **1-TM-Dy**

,
, , , , .
- . . , . .
,
, , , , ,

† Electronic supplementary information (ESI) available: Experimental details, additional characterizations, tables, and figures. CCDC 2088428, 2088429, 2088430 and 2088431. For ESI and crystallographic data in CIF or other electronic format see DOI: 10.1039/d1cc03262c

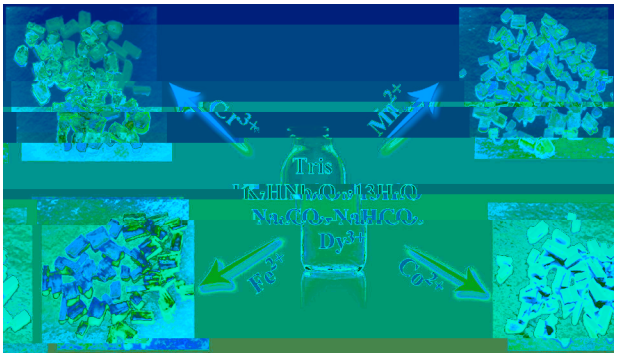

Fig. 1 Crystals morphology of **1-TM-Dy** under an optical microscope and the schematic synthesis process of them.

showed different magnetic properties when different 3d metal ions were introduced.

Single-crystal X-ray diffraction analyses revealed that **1-TM-Dy** are isostructural compounds, and their crystallographic data have been presented in Table S1 (ESI†). In this communication, **1-Cr-Dy** was chosen as an example for the structural description. **1-Cr-Dy** crystallizes in the trigonal system with $\bar{3}1$ space group and its asymmetric unit is composed of a $\{Na_2(H_2O)_3[(Nb_2O_7)CrDyO(\mu_3\text{-}OH)(H_2O)(Nb_3O_{11})]\}$ fragment and sixty-two free water molecules (Fig. S1a, ESI†). The interior of the polyoxoanion is an eight-nuclear Cr–Dy heterometallic cluster $\{Cr_2[Dy_3O(\mu_3\text{-}OH)_3(H_2O)_3]_2\}^{14+}$ (**Cr_2Dy_6**). The structure of **Cr_2Dy_6** can be viewed as a dimer based on two corner-sharing $\{Dy_3O(\mu_3\text{-}OH)_3\}$ clusters and is further capped by two CrO_6 octahedra on both sides along the molecular 3-fold axis (Fig. 2a), resulting in a regular trigonal bipyramid configuration (Fig. 2b). Two **$CrDy_3$** clusters gather together through symmetry operation by Cr1 and Dy1, which are surrounded by the 3-fold axis. Each Cr atom connects to three Dy three μ_3-O (O5), and three Dy atoms connect with each other by a μ_3-O (O2) (Fig. 2c). Furthermore, the **Cr_2Dy_6** cluster is encapsulated by two $\{Nb_6O_{19}\}$ (Nb_6) on both ends and another three **Nb_6** at the equatorial position, respectively (Fig. 2d and e). In detail, six μ_3-(Nb4)–O (O6) atoms are used to connect **Cr_2Dy_6** to **Nb_6** on both ends (Fig. S2a, ESI†). Two μ_3-(Nb1)–O (O8), two μ_3-(Nb2)–O (O3), two μ_2-(Nb2)–O (O4) and one μ_4-(Nb2)–O (O1) are used to connect to **Nb_6** at the equatorial position (Fig. S2b, ESI†). Each Dy^{3+} ion employs a tetragonal antiprism coordination geometry defined by one μ_3-O (O2) shared by three dysprosium atoms, one terminal oxygen (O7), two μ_3-OH (O5, O5a) shared by Cr, three O atoms (O1, O3, O8) from the same equatorial **Nb_6**, and one O4 from another equatorial **Nb_6** (Fig. S2c, ESI†). Bond-Valence Sum (BVS)[11] calculations show that there is one hydroxyl group (O5) ligated by a Cr atom with the BVS values at 1.228, and one terminal H_2O (O7) with the bond valence value at 0.444. The bond distances of Cr–O and Dy–O lie in the range of 1.903–1.915 Å and 2.255–2.433 Å. The oxidation states of Dy1 and Cr1, Mn1, Fe1 and Co1 are +3, +3, +3, +3, +3, respectively (Table S2, ESI†). In addition to Cr^{3+} ions in **1-Cr-Dy**, TM^{3+} ions (Mn^{3+}, Fe^{3+}, Co^{3+}) are observed to be derived from oxidation of TM^{2+} ions because the divalent TM salts are used as the raw materials[5e].[12] To the best of our knowledge, such a series of PONbs containing 3d–4f heterometallic clusters has

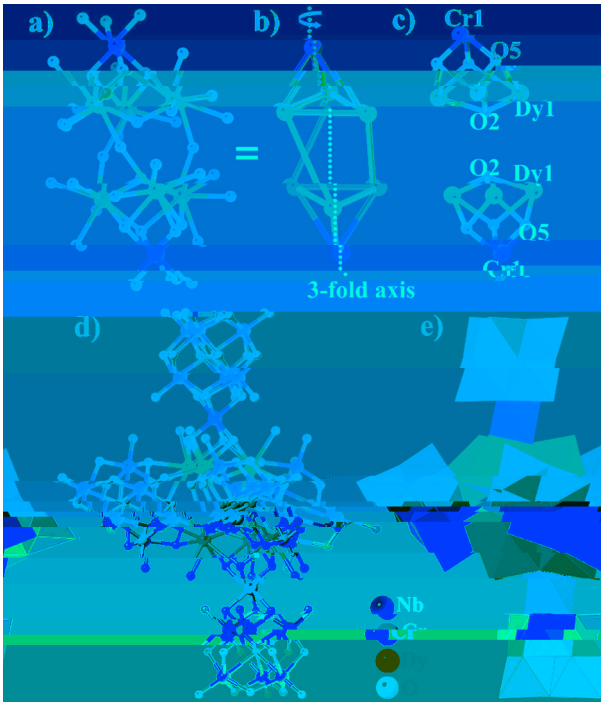

Fig. 2 (a and b) Ball-stick type representation and the simplified version of the 3d–4f heterometallic cluster **Cr_2Dy_6**; (c) the linkage pattern of Cr and Dy by O atoms; (d and e) the ball-stick and polyhedron structure of the polyanion **1-Cr-Dy**. All hydrogen atoms were omitted for clarity. NbO_6 octahedra: red; CrO_8 octahedra: yellow.

not been reported to date, and a similar configuration was only observed in a 3p–4f heterometallic cluster PONb.[13] Interestingly, the charge of the polyoxoanion in **1-Cr-Dy** is balanced by $[Na_6(H_2O)_{24}]^{6+}$. The 3D packing diagram of **1-Cr-Dy** along the axis presents a hexagonal closed-packed structure and the $[Na_6(H_2O)_{24}]^{6+}$ clusters also surrounded the 3-fold axis (Fig. S3, ESI†).

Heterometallic clusters containing transition metals and lanthanide metals might be used as favorable magnetic materials because of the inherent crystal field and contribution effects of 3d and 4f electrons and the interaction between them.[14] The phase purities of **1-TM-Dy** were proved by powder X-ray diffraction characterization (Fig. S4, ESI†). Since **1-TM-Dy** contains different 3d metal ions (Cr^{3+}, Mn^{3+}, Fe^{3+}, Co^{3+}) and lanthanide metal ions (Dy^{3+}), their magnetism was investigated. Direct-current (DC) magnetic susceptibility of **1-TM-Dy** was measured at the temperature of 2–300 K with an external magnetic field of 1 kOe. As shown in Fig. 3a and Fig. S5a–c (ESI†), the experimental (χ_m) values at room temperature are 82.67/86.57/82.68/78.30 cm^3 K mol^{-1}, which are slightly smaller than the theoretical values of 88.77/91.02/93.77/85.02 cm^3 K mol^{-1} expected for two Cr^{3+} ions (= 2, = 3/2)/Mn^{3+} ions (= 2, = 2)/Fe^{3+} ions (= 2, = 5/2)/Co^{3+} ions (= 0) together with six Dy^{3+} ions (= 15/2, = 4/3), probably due to weak antiferromagnetic interactions within the molecules.[7,15] Upon cooling, the values of χ_m decreased gradually to 76.65/81.60/73.06 cm^3 K mol^{-1} at 50 K. With further cooling, the χ_m values witnessed an abrupt decline to the minimum of 58.63/67.52/55.16 cm^3 K mol^{-1} at 2 K for **1-Cr-Dy**, **1-Mn-Dy**, and **1-Co-Dy**, which can be attributed

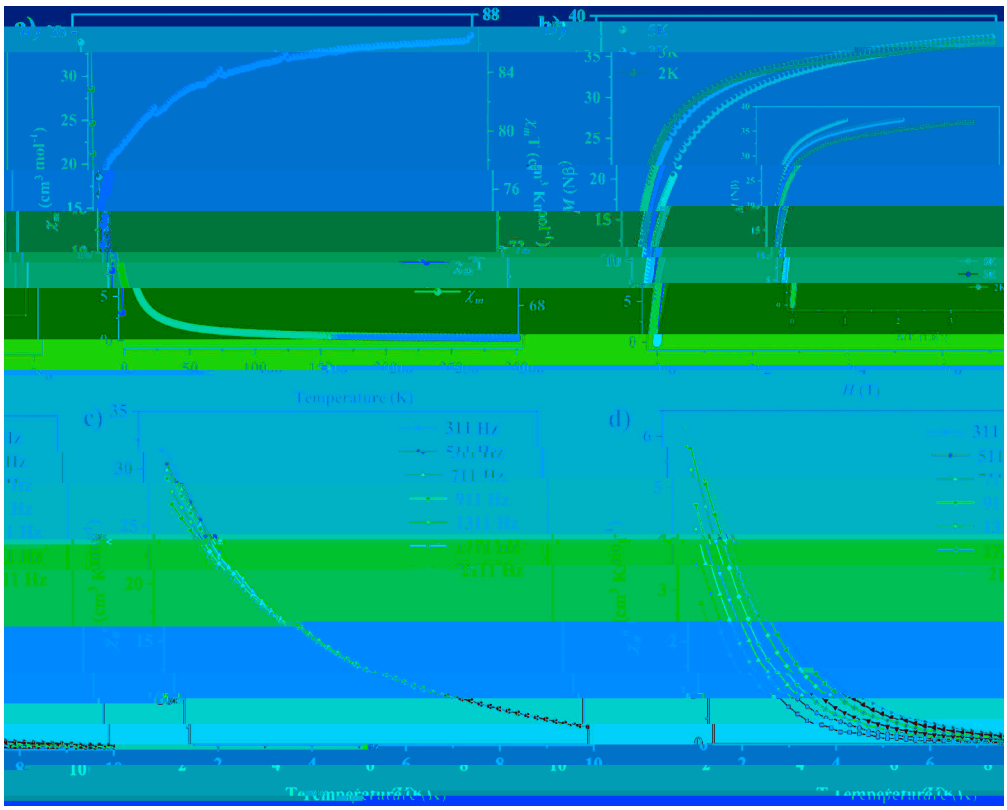

Fig. 3 (a) χ_m *versus T* and $\chi_m T$ *versus* T for **1-Mn-Dy** in the temperature range of 2–300 K; (b) the field dependence of magnetization at 2.0 K, 3.0 K and 5.0 K for **1-Mn-Dy**. Inner: (*M*) *vs.* (*H*/*T*) plots at 2.0 K, 3.0 K, and 5.0 K; (c and d) temperature-dependent behavior of the in-phase (χ_m') and out-of-phase ($\chi m''$) of **1-Mn-Dy** in zero static fields at 2–10 K.

to the obvious antiferromagnetic coupling interaction between the clusters within the clusters and/or the zero-field splitting effect.[7,16] For **1-Fe-Dy**, the χ_m dropped smoothly to 81.26 cm^3 K mol^{-1} at 101 K and then decreased rapidly to the minimum of 78.53 cm^3 K mol^{-1} at 20 K, then followed by a sharp increase to the maximum of 84.33 cm^3 K mol^{-1} at 2 K. This may result from the antiferromagnetism of the clusters in **1-Fe-Dy**.[17] Field-dependent isothermal magnetization (( )) of **1-TM-Dy** was investigated at 2 K, 3 K, and 5 K with a magnetization increase from 0 kOe. As shown in Fig. 3a and Fig. S5d–f (ESI†), the ( ) values increase quickly at low field, reaching 28.53/26.50/29.70/28.99 Nβ at 10 kOe under 2 K, and then climb to the maximum values of 35.48/36.85/38.82/33.33 Nβ, which are smaller than the excepted saturation values of 66/68/70/60 Nβ. This can be attributed to the crystal field effect on the Dy^{3+} ion that removes the degeneracy of the ground state.[18] The nonoverlapping ( ) . (/) for **1-TM-Dy** indicates the existence of significative magnetic anisotropy or low-lying excited states.[19]

In addition, the encapsulation of Mn^{3+} (d^4 electronic configuration, Jahn–Teller distortion) ions in POMs is attractive because of the possibility of single-molecule magnet behavior.[2,20] To further study the dynamic properties of **1-TM-Dy**, alternating-current (ac) magnetic susceptibilities for all compounds with a frequency between 311 and 2111 Hz were measured under an applied magnetic field of 3 Oe and zero DC field. For **1-Mn-Dy**, the observed out-of-phase (χ_m'') signals (about 15% of the in-phase (χ_m') signals) indicate slow relaxation of the magnetization below 10 K. In comparison, the ratios for **1-Cr-Dy**, **1-Fe-Dy**, and **1-Co-Dy** were about 0.58%/0.59%/4.23%, which presented slighter slow relaxation of the magnetization than **1-Mn-Dy** below 8 K (Fig. 3c, d and Fig. S6, ESI†).[21] The out-of-phase (χ_m'') signals of the **1-TM-Dy** show an obvious frequency dependent effect. Besides, no peaks in χ_m'' for **1-TM-Dy** were observed, indicating that such a slow relaxation obeys the Debye model with one energy barrier and one-time constant based on the following relationship (eqn (1))[22]

$$\ln(\chi_m''/\chi_m') = \ln(\omega\tau_0) + \quad / \ _B \qquad (1)$$

For this equation, the Debye model can be used to evaluate the classical slow relaxation process, which can roughly estimate the energy barrier ($_a$/ $_B$) of **1-TM-Dy** (Table S3, ESI†). As a result, **1-Mn-Dy** presents preferable magnetic properties among **1-TM-Dy**, but much smaller than most reported 3d–4f heterometallic compounds (Table S4, ESI†).

In summary, the first series of 3d–4f heterometallic cluster incorporated PONbs **1-TM-Dy** were successfully prepared and characterized. **1-TM-Dy** present different magnetic properties as the incorporated 3d metal ions vary, and all of them reveal significant magnetic anisotropy. Moreover, **1-Mn-Dy** exhibits an obvious and significant slow relaxation of the magnetization. This work not only provides a promising strategy to make new

heterometallic cluster incorporated PONbs but also demonstrates an ideal model to probe how transition-metal ions influence magnetic properties of PONbs.

We gratefully acknowledge the financial support from the National Natural Science Foundations of China (No. 21671040, and 21773029), the Natural Science Fund of Fujian Province (No. 2017J01579), and Projects from the State Key Laboratory of Structural Chemistry of China.

Conflicts of interest

There are no conflicts to declare.

Notes and references

1 ( ) H. N. Miras, J. Yan, D. L. Long and L. Cronin, . . ., 2012, **41**, 7403–7430; ( ) J. Z. Yan, H. F. Su, H. Y. Yang, C. Y. Hu, S. Malola, S. C. Lin, B. K. Teo, H. Hakkinen and N. F. Zheng, ..., 2016, **138**, 12751–12754; ( ) X. X. Li, L. J. Zhang, C. Y. Cui, R. H. Wang and G. Y. Yang, . ., 2018, **57**, 10323–10330; ( ) Z. J. Liu, X. L. Wang, C. Qin, Z. M. Zhang, Y. G. Li, W. L. Chen and E. B. Wang, . . ., 2016, **313**, 94–110; ( ) D. Y. Du, J. S. Qin, S. L. Li, Z. M. Su and Y. G. Li, . . ., 2014, **43**, 4615–4632.

2 ( ) Y. W. Li, Y. G. Li, Y. H. Wang, X. J. Feng, Y. Lu and E. B. Wang, . ., 2009, **48**, 6452–6458; ( ) Y. Z. Chen, Z. J. Liu, Z. J. Liu, Z. M. Zhang, H. Y. Zhou, X. T. Zheng and E. B. Wang, . . ., 2014, **46**, 155–158; ( ) X. K. Fang, K. McCallum, H. D. Pratt III, T. M. Anderson, K. Dennis and M. Luban, ., 2012, **41**, 9867–9870.

3 ( ) O. Oms, A. Dollbecq and P. Mialane, . . ., 2012, **41**, 7497–7536; ( ) S. T. Zheng and G. Y. Yang, . . ., 2012, **41**, 7623–7646; ( ) X. X. Li, Y. X. Wang, R. H. Wang, C. Y. Cui, C. B. Tian and G. Y. Yang, . ., . ., 2016, **55**, 6462–6466; ( ) X. B. Han, Y. G. Li, Z. M. Zhang, H. Q. Tan and E. B. Wang, ..., 2015, **137**, 5486–5493.

4 V. Das, R. Kaushik and F. Hussian, . . ., 2020, **413**, 213271.

5 ( ) Y. N. Gu, H. Yu, L. D. Lin, Y. L. Wu, Z. Li, W. Y. Pan, J. He, L. Chen, Q. Li and X. X. Li, . .